# The Penetration Capacity of a 20 × 102 mm Frangible Armor Piercing Projectile

**Mihaela Badea**
National University of Science and Technology Politehnica Bucharest, Bucharest, Romania
radu.cristianamihaela@gmail.com

**Dragos Gabriel Zisopol**
Department of Mechanical Engineering, Petroleum and Gas University of Ploiești, Ploiești, Romania
zisopold@upg-ploiesti.ro (corresponding author)

**Anton Hadar**
National University of Science and Technology Politehnica Bucharest, Bucharest, Romania
anton.hadar@upb.ro

**Vasile Nastasescu**
Military Technical Academy Ferdinand I, Bucharest, Romania
nastasescuv@gmail.com

*Received: 24 February 2025 | Revised: 31 March 2025 | Accepted: 4 April 2025*

 *DOI: https://doi.org/10.48084/etasr.10708*

## ABSTRACT

**The aim of this work was to evaluate the penetration capacity of armor plates by the 20x102 Frangible Armor Piercing (FAP) projectile. The projectile was numerically modeled using four different variants, each designed to simplify the calculations and avoid the spread of classified information. These variants included the external geometric shape, external dimensions, mass, and impact speed. Deploying the novelty concept of the equivalent bullet (one that preserves the parameters that determine the depth of penetration), this research utilized four different bullet designs. These models were quantitatively evaluated and validated by comparing the numerically predicted penetration performance with the experimental testing results. The results led to errors just below 1%, except Model-4 which exceeded 30%. This work is useful not only to researchers in the field of terminal ballistics, but also in a general filed of researchers engaged in Finite Element Method (FEM).**

***Keywords-bullet; armor plate; impact; finite element method; material model***

## I. INTRODUCTION

The effect of solid bodies with different speeds has been investigated over the years, with different technologies being employed for this purpose. Researchers from both military and civil fields, such as aircraft manufacturers and others, have contributed to this issue [1].

The range of impact speeds depends on their applications. In the case of automotive industry, speed ranges from tens of m/sec, while in the case of non-lethal or self-defense weapons, speed ranges from tens and hundreds of m/sec. In the case of individual weapons, from hundreds of m/sec, as well as in the case of large-caliber designed to penetrate armored vehicle weapons, speed is around 1000 m/s. Additionally, projectiles with high penetrating power can reach speeds from 1500 to 2000 m/s and in the case of impact with meteorites, speeds may be in the order of tens of km/s. Although exceptions are not excluded, and the field of impact speeds is neither complete nor strictly defined, this range presents the diversity of scenarios involving solid body effects [2].

Over time, an engineering discipline known as terminal ballistics appeared and was developed, in step with the new means of combat, as well as with the calculation and experimental investigation of the impact phenomenon. High impact speeds, typically from hundreds of m/sec, require a special approach, based on theories, including elasticity, plasticity, hydrodynamics, high pressure physics, fracture mechanics, viscoplasticity, viscoelasticity, and the development of specific criteria, beyond the resistance of the materials, of the transfer of the material. At such velocities, the damage induced in the target is highly localized, with a lateral extent greater than a few projectile diameters, but is concentrated along the direction of projectile motion.

Specialists in the field of projectile-target impact can be separated into two categories according to the objectives pursued: those focused on increasing the projectile penetration or perforation capacity by adjusting certain mass, speed, geometric characteristics, materials, and constructive solutions, and those who deal with enhancing the protection capacity of the target represented by the armor plate. These efforts involve optimizing some materials (composites, ceramics, etc.), geometric shapes, physical characteristics, and behavior at high speed deformations. The most commonly used method for simulating projectile-target impacts is the FEM [3]. However, newer techniques have been developed, such as the meshfree (e.g., Galerkin-free element method) and meshless (e.g., smoothed particle hydrodynamics) methods. All these can be applied individually or in combination to achieve the optimal results [4, 5].

In numerical modeling, more or less attention (without leading to a distortion of the results) is given to the armor plate or the projectile modeling [6]. This selective approach, when validated experimentally, helps to save time and resources [7]. According to this concept, the present paper proposes finite element models of projectiles that reduce computational complexity without affecting the accuracy of target behavior predictions. FAP projectile is studied, with a caliber of 20 mm × 102.25 mm [8]. Due to their special design, FAP projectiles do not ricochet. Instead, their cores disintegrate upon impact. The proposed models are compatible with both FEM and meshfree/meshless methods [9].

## II. KINETIC PROJECTILE COMPONENTS

The bullet or, more generally, the projectile exhibits a more complex structure, particularly as caliber increases. The components of projectiles also depend substantially on the object type. Figure 1 illustrates a typical projectile, though dimensions and components may differ across various projectiles [10-12].

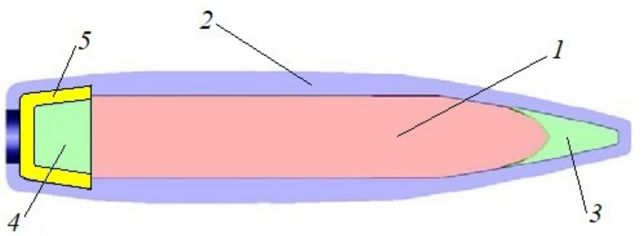


Fig. 1. Typical components of a kinetic armor-piercing projectile. These iclude: 1-bullet (hard) core, 2-bullet jacket, 3-point filler, 4-base filler, 5-bullet cover.

In this research, the numerical models and experimental tests relied on a 20 mm FAP projectile, as depicted in Figure 2. However, both experimental and numerical research on the impact of such projectiles usually considers the projectile's external geometry, dimensions, and shape, neglecting the internal construction details of the bullet itself [13]. The optimum numerical model is the one that respects in detail all the properties of a real bullet. Such detailed modeling is not always feasible due to various limitations; thus, a model similar to the one shown in Figure 2(a) can be used. Starting from the constructive data in Figure 2(b), some bullet numerical models were adopted [14, 15]. The two basic geometrical models utilized in this study are presented in Figures 3 and 4. The first model (Figure 3) is the one that faithfully describes the real component of the bullet, being the so-called real model. The second model (Figure 4) is quite similar to the one in Figure 1, with the same components, respecting the dimensions, shape, and weight (mass) of the real bullet (105 ± 2 g). Utilizing these two base geometries, FEM variants of the projectile were developed, which were then employed in simulations of normal impact scenarios, using both 2D axial-symmetric models and simplified 3D models (reduced to one quarter due to symmetry in normal impact conditions).

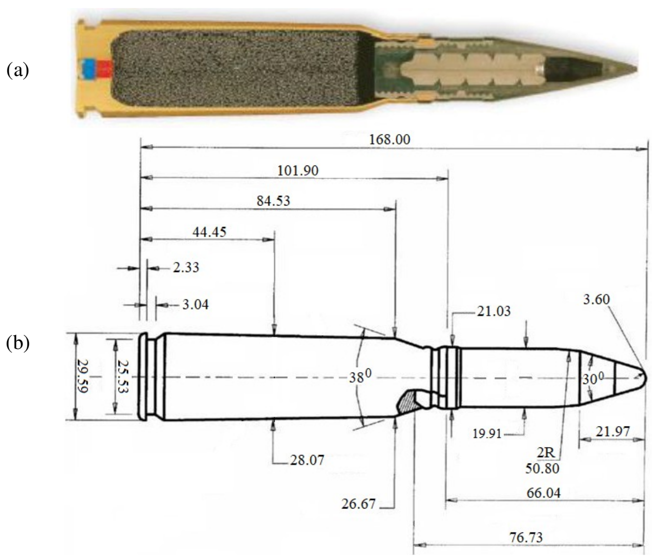


Fig. 2. (a) Longitudinal section through a cartridge with FAP, (b) main dimensions of the FAP cartridge.

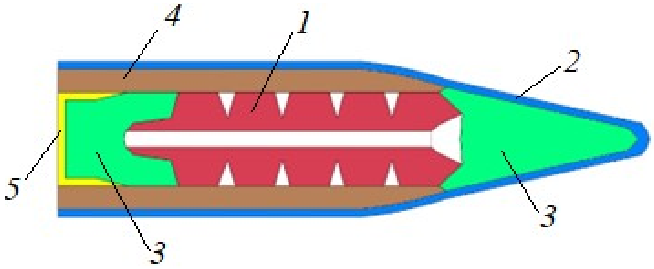


Fig. 3. Longitudinal section through a real bullet. Its components are: 1-frangible hard (bullet) core, 2-bullet jacket, 3-bullet filler, 4-bullet body, 5-bullet cover.

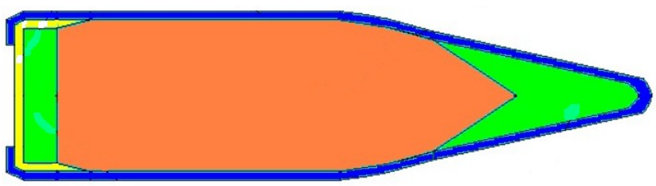

Fig. 4. Longitudinal section through an equivalent bullet.

## III. BULLET FINITE ELEMENT MODELS

The axially symmetric 2D model is highly efficient as it significantly reduced the number of nodes and elements, and consequently the number of equations, leading to a lower computer time [16, 17]. In the utilized software, these models are defined as flat with uneven thickness, corresponding to an opening angle at the center of 1 radian [16-18]. Thus, the volume and mass of the respective model can be calculated. Figures 5 and 6 provide examples of such 2D FEMs. These are shell type elements, with the option of axial-symmetric behavior, using 3 and 4 nodes [18]. The model in Figure 5 was named Model-1and the one in Figure 6 was called Model-2. The main characteristics of these 2D models are presented in Table I. For both FEM approaches, the finite element size did not exceed 2 mm. This limitation was chosen because the focus of the study lies on the behavior of the bullet rather on its effect on the target. The simplified FEM/Finite Element models (due to symmetry) for the 3D real model are presented in the Figures 7 and 8, for the normal impact [19] (Also called Model-3 and Model-4, respectively.)

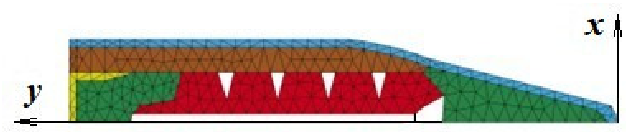


Fig. 5. Real bullet 2D finite element model.

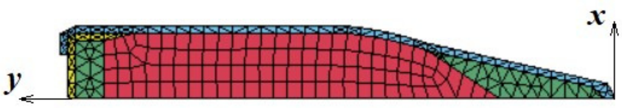


Fig. 6. Equivalent bullet 2D finite element model.

TABLE I. CHARACTERISTICS OF BULLET MODELS

| Bullet model | Bullet components | 2D | | 3D | |
|---|---|---|---|---|---|
| | | Finite element number | Node number | Finite element number | Node number |
| Model-1 | Core | 119 | 92 | 366 | 637 |
| | Jacket | 103 | 94 | 252 | 569 |
| | Filler | 111 | 85 | 306 | 445 |
| | Body | 104 | 82 | 288 | 539 |
| | Cover | 17 | 18 | 54 | 107 |
| | Total | 454 | 371 | 1266 | 2297 |
| Model-2 | Core | 105 | 136 | 2753 | 4519 |
| | Jacket | 114 | 102 | 1992 | 3941 |
| | Filler | 62 | 53 | 532 | 1101 |
| | Cover | 32 | 27 | 415 | 853 |
| | Total | 313 | 318 | 5692 | 10414 |

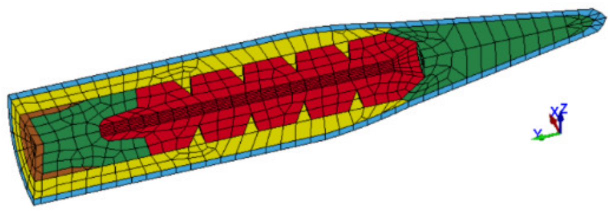

Fig. 7. A 3D finite element real model – quarter of the structure.

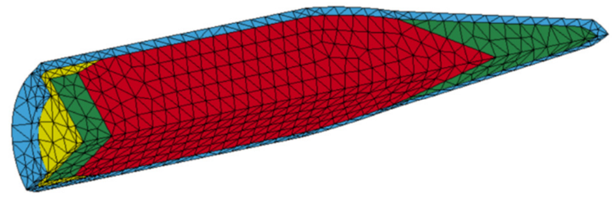

Fig. 8. A 3D finite element model of the bullet - quarter of the structure.

The four variants of bullet modeling are summarized in Table II. Models 2-4 share the same finite element construction as Model-1 but differ in the adopted material models.

TABLE II. VARIANTS OF BULLET MODELING

| Bullet models | Characteristics |
|---|---|
| Model-1 | All components of the real bullet are modeled with finite elements, based on their actual geometry, dimensions, and materials. |
| Model-2 | The material properties are real, except for the bullet core, where the density was calculated to maintain the real total weight, as specified by the supplier. |
| Model-3 | The material properties are real, except for the bullet core, where the density was calculated to maintain the real total weight, as specified by the supplier. |
| Model-4 | The material properties are real, except for the bullet core, where the density was calculated to maintain the real total weight, as specified by the supplier. |

For the axisymmetric 2D models, the volumes and masses of the components, as well as their total values, are presented in Table III, and the details for the 3D models are presented in Table IV.

TABLE III. 2D COMPONENTS: MASSES AND VOLUMES

| Model type | 2D Finite element model | | | |
|---|---|---|---|---|
| | Parts | Volume ($m^3$) | Mass per radian (kg/rad) | Mass (kg) |
| Model-1 | Core | 3.50977E-06 | 0.00863033 | 0.05422600 |
| | Jacket | 3.55988E-06 | 0.00504249 | 0.03168290 |
| | Filler | 2.54411E-06 | 0.00030384 | 0.00190910 |
| | Body | 6.32784E-06 | 0.00271919 | 0.01708520 |
| | Cover | 3.22537E-07 | 4.10872E-05 | 0.00025816 |
| | Total | 1.62641E-05 | 0.016737 | 0.105161 |
| Model-2 | Core | 1.10535E-05 | 0.011259000 | 0.07074230 |
| | Jacket | 3.71545E-06 | 0.005298340 | 0.03329040 |
| | Filler | 1.68415E-06 | 0.000222582 | 0.00139852 |
| | Cover | 5.57154E-07 | 0.000073635 | 0.00046266 |
| | Total | 1.70103E-05 | 0.016854 | 0.105894 |
| Model-3 | Equivalent density: 6,172.747 kg/$m^3$ | | | 0.104998 |
| Model-4 | | | | |

## IV. EXPERIMENTAL INVESTIGATIONS

The experimental research is based on a series of firings into armor plates using the ballistic barrel, as depicted in Figure 9(a), on the M621 gun loaded with 20 mm × 102 mm ammunition. These plates were made of steel with a height of 250 mm, width of 250 mm, and a thickness of 23 mm. The armor plates (target) were fixed in a special device designed for experimental tests, as presented in the Figure 9(b). Besides this equipment, an ultra-fast filming PHOTRON FASTCAM SA-Z, portrayed in Figure 9(c), of the impact process was used [20].

TABLE IV. 3D COMPONENTS, MASSES, AND VOLUMES

| Model type | 3D Finite element model | | | |
|---|---|---|---|---|
| | Parts | Volume ($m^3$) | Mass per radian (kg/rad) | Mass (kg) |
| Model-1 | Core | 8.68591E-07 | 0.01383230 | 0.055329 |
| | Jacket | 8.79207E-07 | 0.00769306 | 0.030772 |
| | Filler | 6.28842E-07 | 0.00047188 | 0.001888 |
| | Body | 1.56186E-06 | 0.00420141 | 0.016806 |
| | Cover | 7.99104E-08 | 6.39603E-05 | 0.000256 |
| | Total | 4.01841E-06 | 2.62626E-02 | 0.105050 |
| Model-2 | Core | 2.76414E-06 | 0.0170624 | 0.0682496 |
| | Jacket | 9.29165E-07 | 0.0057355 | 0.0229420 |
| | Filler | 4.20923E-07 | 0.0025983 | 0.0103932 |
| | Cover | 1.39289E-07 | 0.0008598 | 0.0034392 |
| | Total | 4.25352E-06 | 0.0262560 | 0.105024 |
| Model-3 | Equivalent density: 6,172.747 kg/$m^3$ | | | 0.105023 |
| Model-4 | | | | |

(a)
(b)
(c)

Fig. 9. Experimental devices.

The experimental results are presented in the Table V.

TABLE V. EXPERIMENTAL RESULTS

| Materia l target | Impact velocity (m/s) | Residual velocity (m/s) | Maximum diameter of the hole (mm) | |
|---|---|---|---|---|
| | | | Impact face | Back face |
| Steel | 1092.780 | 655.670 | 26.0 | 25.0 |

The impact and residual velocities were automatically determined by the camera through a dedicated software. These speed values are displayed in Figure 10. An interesting aspect is also illustrated, characteristic of frangible armor piercing projectiles. It is about the phenomenon of the disintegration of the bullet core. After piercing the target, the heavy metal pellets (bullet core) disintegrate into multiple fragments [13, 21].


Fig. 10. Automatic recording of the result in the polygon.

## V. NUMERICAL MODELING OF THE IMPACT

The effects of the four numerical bullet modeling variants were investigated in comparison with the experimental results. Among the modeling approaches, the 2D axisymmetric (planar) model proved to be the most efficient, as it leads to the lowest number of nodes and elements and, consequently, to the smallest number of equations. Two commonly employed material models from LS-DYNA material library were deployed in this study: the Plastic-Kinematic model and the Rigid material model [22, 23].

In the 2D axisymmetric model, the target was modeled using 4-node finite elements, with a variable mesh density ranging from 0.5 to 2 mm [24]. The mesh consisted of 1,449 elements and 1,536 nodes. The 3D simplified model (quarter of the structure) is modeled with finite elements of 8 nodes, with a variable network, as in 2D modeling. The finer elements were collected in the impact area [5, 24, 25].

The same materials and material models were used for both 2D and 3D models. The real bullet models (Figures 5 and 7) and the equivalent models (Figures 6 and 8) are composed by the following materials, as presented in Table VI.

From the material library of software LS-DYNA [9], the MAT_003 (Plastic-Kinematic) and MAT_020 (Rigid) models were employed for the bullet components. In contrast, for the armor plate (target), only MAT_003 (Plastic-Kinematic) was used. The Cowper Symonds strain rate parameters applied were $C$ = 40 and $p$ = 5.00 for steel and tungsten alloy, while the values for the aluminum were $C$ = 6500 and $p$ = 4.00.

TABLE VI. MATERIAL ELASTIC PROPERTIES

| Materials | Young µodulus, *E* (Pa) | Poisson rate ($\nu$) | Density, $\rho$ (kg/m$^3$) |
|---|---|---|---|
| Steel | $2.1 \cdot 10^{11}$ | 0.30 | 7850 |
| Aluminum | $0.7 \cdot 10^{11}$ | 0.34 | 2700 |
| Tungsten alloy | $2.05 \cdot 10^{11}$ | 0.30 | 15450 |
| Brass | $1.38 \cdot 10^{11}$ | 0.33 | 8330 |
| Filler | $2.75 \cdot 10^{9}$ | 0.43 | 750 |

## VI. COMPARATIVE RESULTS

The results of the numerical impact simulations are presented in comparison with the experimental results in Table VII.

TABLE VII. COMPARATIVE RESULTS FOR DIFFERENT BULLET MODELS

| Bullet models | Residual velocity (FEM) (m/s) | Residual velocity (experiment) (m/s) | Percentage error (%) |
|---|---|---|---|
| 1 | 656.00 | 655.670 | 0.05 |
| 2 | 652.00 | | -0.56 |
| 3 | 652.00 | | -0.56 |
| 4 | 879.00 | | 34.06 |

Figures 11-14 illustrate the numerical results obtained from those four bullet models, including: (a) the impact modeling, (b) the evolution of bullet velocity, and (c) the deformed states of both bullet and target at a given time during perforation. From these findings, it can be concluded that Model 1, which uses real geometry and real properties, is the most appropriate simulation of the impact behavior. Notably, as shown in Figure 11, the bullet core fragmentation phenomenon is very well modeled [14, 26].

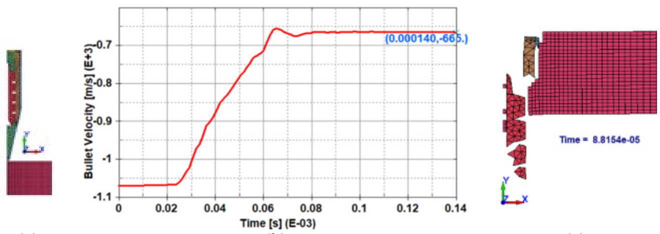


(a) (b) (c)

Fig. 11. Numerical results with bullet Model-1.

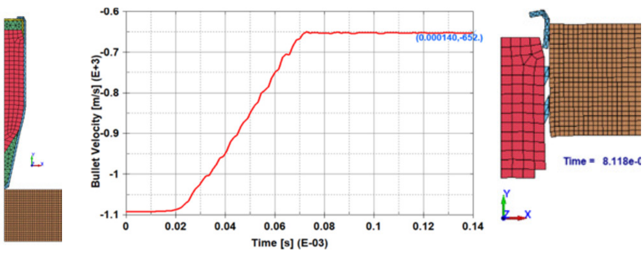


(a) (b) (c)

Fig. 12. Numerical results with bullet Model-2.

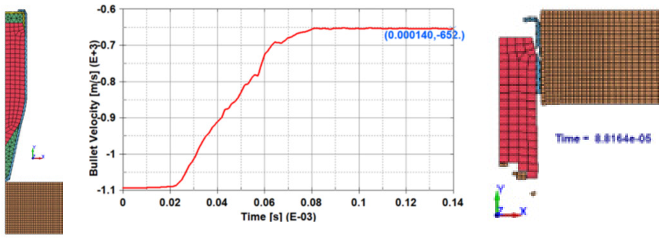


(a) (b) (c)

Fig. 13. Numerical results with bullet Model-3.

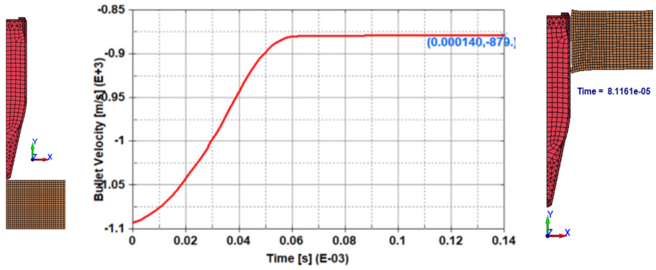


(a) (b) (c)

Fig. 14. Numerical results with bullet Model-4.

While 3D models significantly require more computational time, their results are fully consistent with those obtained using 2D finite element models and, more importantly, fully consistent with the experimental results. Figure 15 porytrays the phenomenon of bullet fragmentation of the frangible bullet using the 3D finite element model on Model-1. This aspect can only be simulated with Model 1, regardless of 2D (Figure 11(c)) or 3D modeling (Figure 15).

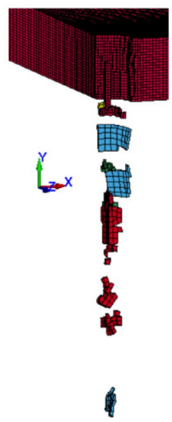

Fig. 15. The bullet fragmentation simulation by the 3D model.

## VII. CONCLUSIONS

The aim of this study was to assess the penetration capability of armor plates by the 20 × 102 mm Frangible Armor Piercing (FAP) projectile. The projectile was modeled using four bullet models, each designed for different practical needs. The novelty of this paper lies in the introduction of the equivalent bullet concept, represented by bullet Models 2 and 3, both used in 2D and 3D modeling. All four models are compatible with the Finite Element Method (FEM), as well as with alternative numerical approaches, such as meshfree and meshless methods. These models were quantitatively evaluated and validated by comparing the numerically predicted penetration performance with results from experimental testing. The numerical models achieved errors of less than 1%, with none exceeding 4%. The use of equivalent bullet models (Model-2 and Model-3) is a valid solution, offering an ease of modeling and reduced computer time. In contrast, the use of the rigid material model (bullet Model-4) could be a solution for some precautions, such as a good calibration of the model if some results are known. Otherwise, the errors can rise to even 30%. The outcomes of this work provide a validated and practical methodology for modeling high-velocity projectile impacts and are applicable not only to specialists in terminal ballistics, but also to a broader range of researchers engaged in finite element modeling of impact phenomena.

## REFERENCES

[1] R. McCoy, Modern exterior ballistics: The launch and flight dynamics of symmetric projectiles, 2nd ed. Schiffer Military History, 2012.

[2] Z. Rosenberg and E. Dekel, *Terminal Ballistics*. Berlin, Germany: Springer, 2012.

[3] G. Ben-Dor, A. Dubinsky, and T. Elperin, "Method of basic impactors for simplified modeling of penetration," *Engineering Fracture Mechanics*, vol. 76, no. 4, pp. 614–618, Mar. 2009, https://doi.org/10.1016/j.engfracmech.2008.10.007.

[4] M. McTee, C. N. Parish, C. Jourdonnais, and P. Ramsey, "Weight retention and expansion of popular lead-based and lead-free hunting bullets," *Science of The Total Environment*, vol. 904, Dec. 2023, Art. no. 166288, https://doi.org/10.1016/j.scitotenv.2023.166288.

[5] A. Mukhtar and H. Nasir, "Comparative closed vessel firing-ballistic parameters evaluation for development of base bleed composite solid propellant," *Engineering, Technology & Applied Science Research*, vol. 8, no. 6, pp. 3545–3549, 2018, https://doi.org/10.48084/etasr.2370.

[6] A. Morka, B. Jackowska, and T. Niezgoda, "Numerical study of the shape effect in the ceramic based ballistic panels," *Journal of KONES*, vol. Vol. 16, No. 4, pp. 539–548, 2009.

[7] R. Laible, *Ballistic Materials and Penetration Mechanics*. Amsterdam, Netherlands: Elsevier, 2012.

[8] O.-E. Vlas, "20 mm Frangible Armour Piercing Projectile." Military Technical Academy.

[9] *LS-DYNA, Keyword User's Manual Volume I,* Livermore Softwate Technology Corporation (LSTC), Livermore, CA, USA, Aug, 2012.

[10] V. Năstăsescu, "Impact Estimation Between Armour and Kinetic Projectiles," *Proceedings of the Romanian Academy,* no. 3, 2000.

[11] B. P. Kneubuehl, *Ballistics: Theory and Practice*. Berlin, Germany: Springer Nature, 2024.

[12] O. Lynch, *The Sicence of Ballistics*. New York, NY, USA: Clanrye International, 2018.

[13] "30mm Armor-Piercing Ammunition," Defence Update. https://defense-update.com/20060602_30mm-ap.html#.VT541SGqqko.

[14] P. P. Massaro, *Big Book of Ballistics*. Iola, WI, USA: Gun Digest, 2017.

[15] G. Klimi, *Exterior Ballistics: The Remarkable Methods*, 1st ed. Bloomington, IN, USA: Xlibris, 2014.

[16] K.-J. Bathe, *Finite Element Procedures*, 2nd ed. Hoboken, NJ, U.S.A.: Prentice Hall, 1996.

[17] O. C. Zienkiewicz, R. L. Taylor, and J. Z. Zhu, *The Finite Element Method: Its Basis and Fundamentals*, 6th ed. Amsterdam, Netherlands: Elsevier, 2005.

[18] *LS-DYNA Theory Manual*, Livermore Softwate Technology Corporation (LSTC), Livermore, CA, USA, Mar. 2006.

[19] G. I. Balan, D. G. Zisopol, A. Stefan, V. Nastasescu, and L. Grigore, "Study of the Injection of Secondary Air into the Intake Manifold of the Gas Turbine to Avoid the Compressor Surging Phenomenon," *Engineering, Technology & Applied Science Research*, vol. 14, no. 2, pp. 13248–13254, Apr. 2024, https://doi.org/10.48084/etasr.6927.

[20] T. Børvik, M. Langseth, O. S. Hopperstad, and K. A. Malo, "Ballistic penetration of steel plates," *International Journal of Impact Engineering*, vol. 22, no. 9, pp. 855–886, Oct. 1999, https://doi.org/10.1016/S0734-743X(99)00011-1.

[21] R. G. O'Donnell, "An investigation of the fragmentation behaviour of impacted ceramics," *Journal of Materials Science Letters*, vol. 10, no. 12, pp. 685–688, Jan. 1991, https://doi.org/10.1007/BF00722768.

[22] V. Nastasescu and M. Bunea, "Some Material Models Used in Finite Element Analysis of the Impact Problems," *5th International Armament Conference,* Warsaw, Poland, 06-08 October, 2004, , pp. 721-729.

[23] V. Narayanamurthy, C. L. Rao, and B. N. Rao, "Numerical simulation of ballistic impact on armour plate with a simple plasticity model," *Defence Science Journal*, vol. 64, no. 1, Art. no. 55, Jan. 2014.

[24] E. A. Flores-Johnson, M. Saleh, and L. Edwards, "Ballistic performance of multi-layered metallic plates impacted by a 7.62-mm APM2 projectile," *International Journal of Impact Engineering*, vol. 38, no. 12, pp. 1022–1032, Dec. 2011, https://doi.org/10.1016/j.ijimpeng.2011.08.005.

[25] A. Malciu, C. Pupăză, C.-C. Puică, and I.-F. Pană, "Finite element model validation for a 14.5 mm armor piercing bullet impact on a multi-layered add-on armor plate," *MATEC Web of Conferences*, vol. 373, 2022, Art. no. 00038, https://doi.org/10.1051/matecconf/202237300038.

[26] N. Kılıç, S. Bedir, A. Erdik, B. Ekici, A. Taşdemirci, and M. Güden, "Ballistic behavior of high hardness perforated armor plates against 7.62 mm armor piercing projectile," *Materials & Design*, vol. 63, pp. 427–438, Nov. 2014, https://doi.org/10.1016/j.matdes.2014.06.030.